

# Contents

<b>1</b>	<b>Introduction</b>	<b>2</b>
<b>2</b>	<b>Non-divergent Vector Fields</b>	<b>2</b>
<b>3</b>	<b>Unconditional simulation</b>	<b>3</b>
3.1	Differentiation of a simulated scalar field . . . . .	3
3.2	Direct simulation of the vector field . . . . .	4
<b>4</b>	<b>Conditional simulation</b>	<b>5</b>
<b>5</b>	<b>Examples</b>	<b>8</b>
5.1	Unconditional simulation . . . . .	8
5.2	Conditional simulation . . . . .	10
<b>6</b>	<b>Verification of the program by simulation</b>	<b>21</b>
<b>7</b>	<b>Conclusions</b>	<b>25</b>
<b>8</b>	<b>References</b>	<b>25</b>

# 1 Introduction

NSPACE is a package for methods in spatial statistics, implemented in C++. In this note, we present the methods for unconditional and conditional simulation of nondivergent, isotropic vector fields, that are implemented.

In section 2, a definition of nondivergent vector fields is given. In section 3 and 4, the methods for unconditional and conditional simulation are presented, and in section 5 some examples are given. A verification of the methods by simulation is presented in section 6. Some concluding remarks are given in section 7.

The work is supported by The Research Council of Norway through the research program no. STP 28402: “Toolkits in Industrial Mathematics”.

## 2 Non-divergent Vector Fields

Let  $\mathbf{V}(\mathbf{x}) = U(\mathbf{x}) \mathbf{i} + V(\mathbf{x}) \mathbf{j}$  be a spatial random vector field in 2-D. It is easily verified that this vector field will be non-divergent ( $\nabla \cdot \mathbf{V} = 0$ ) if it is related to a random scalar field  $\Psi(\mathbf{x})$  through:

$$(1) \quad U(\mathbf{x}) = -\frac{\partial \Psi}{\partial y}, \quad V(\mathbf{x}) = \frac{\partial \Psi}{\partial x}.$$

The non-divergence property of  $\mathbf{V}(\mathbf{x})$  is typical for vector fields representing the velocity field of an incompressible fluid, and in this case  $\Psi(\mathbf{x})$  is called a *stream function*.

To specify the covariance matrix  $F_{\mathbf{V}}(r, \theta)$  of a homogeneous, isotropic non-divergent vector field, it is sufficient to specify a differentiable covariance function for the longitudinal component  $F_{v_r v_r}$  (see Høst (1994)):

$$(2) \quad F_{\mathbf{V}}(r, \theta) = (F_{v_r v_r}(r) - \frac{d}{dr} (r F_{v_r v_r})) \frac{1}{r^2} \mathbf{r} \mathbf{r}' + \frac{d}{dr} (r F_{v_r v_r}) \mathcal{I},$$

where  $\mathbf{r} = r \cos \theta$  and  $V_r$  is the component of  $\mathbf{V}$  along the direction of  $\mathbf{r}$ . Høst (1994) also showed that  $F_{\mathbf{V}}$  can be expressed in terms of a twice differentiable covariance function  $F_{\Psi}$  for the scalar field  $\Psi$ :

$$(3) \quad F_{\mathbf{V}}(r, \theta) = - \left( \frac{1}{r} \frac{dF_{\Psi}}{dr} - \frac{d^2 F_{\Psi}}{dr^2} \right) \frac{1}{r^2} \mathbf{r} \mathbf{r}' - \frac{d^2 F_{\Psi}}{dr^2} \mathcal{I}.$$

Properties of the covariance matrix  $F_{\mathbf{v}}$  are most easily expressed in longitudinal ( $V_r$ -) or transversal ( $V_\theta$ -) components, and by isotropy these two components are uncorrelated. Further details and properties of random 2-D velocity fields, as well as some references, are given in Høst (1994).

### 3 Unconditional simulation

The routines for unconditional simulation are based on the specification of a non-divergent random vector field, as described in section 1. Two algorithms are implemented in NSPACE. In the first algorithm, the vector field is computed from numerical differentiation of the corresponding simulated scalar field  $\Psi$ . In the second algorithm, the vector field is simulated directly from a specification of the structure of covariance and cross-covariance of the components of the field.

#### 3.1 Differentiation of a simulated scalar field

Equation (1) suggests a two-step procedure for simulating the vector field. At the first stage, a scalar field is simulated according to the specification of the covariance structure of the field. At the second stage, the corresponding non-divergent vector field is computed by numerical differentiation.

We assume that the scalar field  $\Psi$  is simulated on a grid lattice. The components  $U_{i,j}$  and  $V_{i,j}$  of the vector field  $\mathbf{V}$  are computed by

$$(4) \quad \begin{aligned} U_{i,j} &= -\frac{\Psi_{i,j+1} - \Psi_{i,j}}{\Delta x_2}, \\ V_{i,j} &= \frac{\Psi_{i+1,j} - \Psi_{i,j}}{\Delta x_1}. \end{aligned}$$

Here,  $\Psi_{i,j}$  is the simulated value of the scalar field in the grid lattice point  $(i, j)$ , and  $\Delta x_1$  and  $\Delta x_2$  are the grid spacings in the two coordinate directions.

To achieve values for the vector field at the boundaries, the scalar field is simulated in a grid augmented by one grid unit outside the original simulation domain.

#### Simulation of a scalar field

Let  $\mathbf{x}_1, \dots, \mathbf{x}_n$  be the coordinates of a set of points in  $\mathcal{R}^2$ . A random scalar field  $\Psi(\mathbf{x})$  is simulated at  $n$  locations by drawing from a multinormal distribution,  $\Psi \sim N(\boldsymbol{\mu}, \boldsymbol{\Sigma})$ , where  $\boldsymbol{\mu} = (\mu_1, \dots, \mu_n)'$  and  $\boldsymbol{\Sigma} = ((Cov(\mathbf{x}_i, \mathbf{x}_j))_{i,j=1, \dots, n})$ .

The field is assumed to be stationary and isotropic, implying that the covariance function depends on the radial distance only:

$$(5) \quad \text{Cov}(\mathbf{x}_1, \mathbf{x}_2) = C(\|\mathbf{x}_1 - \mathbf{x}_2\|) = C(r).$$

A vector  $\mathbf{w}$  of numbers from the standard normal distribution,  $\mathbf{w} \sim N(\mathbf{0}, \mathbf{I})$  is simulated, and the scalar field is computed by

$$(6) \quad \Psi = \mathbf{L}\mathbf{w} + \mu,$$

where  $\mathbf{L}$  is the Cholesky factor of  $\Sigma$ .

For locally smooth fields, characterized by a highly differentiable covariance function, the Cholesky decomposition might fail because of numerical instability. This instability is resolved by adding a small number to the diagonal element of  $\Sigma$  when the decomposition reaches a non-positive pivot element.

### 3.2 Direct simulation of the vector field

To simulate directly from the joint distribution of the components of the vector field, we need to specify the covariance and cross-covariance functions of the components. For a non-divergent, two-dimensional, isotropic vector field, these can be computed from a scalar covariance function, as explained in section 2. To get valid covariance functions, the corresponding scalar covariance function  $C(r)$  must be twice differentiable for all  $r$ .

The field is simulated by a direct generalization of the scalar simulation described in section 3.1, replacing  $\Psi$  by

$$(7) \quad \mathbf{Y} = \begin{pmatrix} \mathbf{U} \\ \mathbf{V} \end{pmatrix},$$

where  $\mathbf{U}$  and  $\mathbf{V}$  are length  $n$  vectors of simulated values for the  $U$ - and  $V$ -components of the vector field in the  $n$  points of the simulation domain.

The vector field is simulated from a multinormal distribution,  $\mathbf{Y} \sim N(\boldsymbol{\mu}_Y, \Sigma_Y)$  where

$$(8) \quad \boldsymbol{\mu}_Y = \begin{pmatrix} \boldsymbol{\mu}_U \\ \boldsymbol{\mu}_V \end{pmatrix},$$

and the covariance matrix  $\Sigma_Y$  of  $\mathbf{Y}$  is given by

$$(9) \quad \Sigma_Y = \begin{pmatrix} \Sigma_{UU} & \Sigma_{UV} \\ \Sigma_{VU} & \Sigma_{VV} \end{pmatrix}.$$

The simulation is carried out as for a scalar field, replacing  $\boldsymbol{\mu}$  and  $\boldsymbol{\Sigma}$  in section 3.1 with  $\boldsymbol{\mu}_Y$  and  $\boldsymbol{\Sigma}_Y$ .

An advantage of this method is that we can simulate for irregularly spaced points, as well as for points on a grid lattice. But numerical problems might arise if the points of the simulation domain are very close and the covariance function is smooth, causing a (numerically) non-positive definite covariance matrix. As mentioned for the scalar simulation in section 3.1, a modified Cholesky decomposition is used in these cases, but this leads to approximate solutions.

The covariance function

$$(10) \quad c(r) = c_0 e^{-3\left(\frac{r}{R}\right)^2},$$

where  $c_0$  is the variance and  $R$  the range, is a typical example. This model is not desirable, because it is infinitely many times differentiable.

By choosing carefully among the valid covariance models, one can reduce this instability. But for the non-divergent vector field as defined in (1), the number of available covariance models are limited, since the covariance function is required to be twice differentiable.

A good choice is a model based on modified Bessel functions. The longitudinal and transversal components of this model, as well as for the “gaussian” type model defined in (10), are printed in figure 1. Examples of simulations using both models are shown in section 5.

Another problem is that the Cholesky decomposition method is computationally expensive, and has shown to be stable only for a relatively small number of points. The covariance matrix will be of dimensions  $(2N_x N_Y \times 2N_x N_Y)$ , increasing rapidly with the number of grid points.

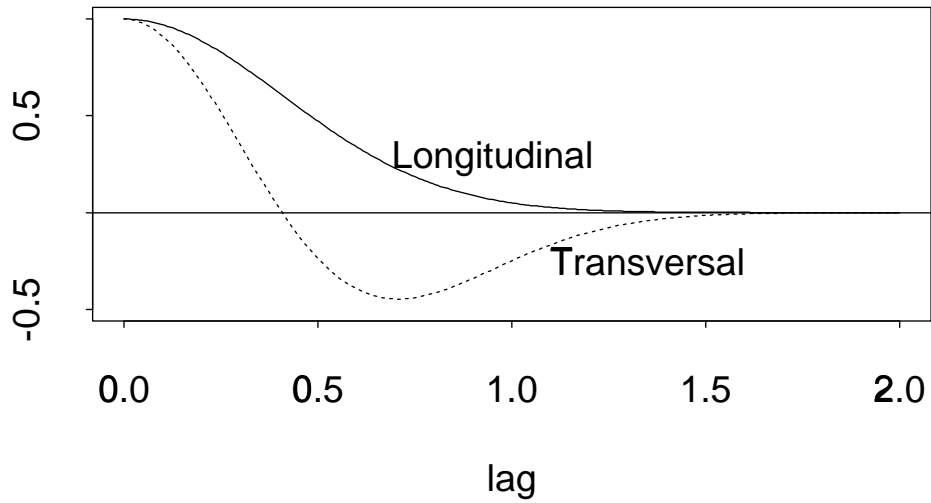
## 4 Conditional simulation

A conditional simulation of a random field given data is a realisation of the field constrained to reproduce the data at the data locations. For an isotropic scalar field  $\Psi$ , we can show that the isotropic scalar field and a non-divergent vector field are always uncorrelated (Høst, 1994). Therefore, we can not use the scalar field approach of section 3.1 for conditional simulation.

The method implemented in NSPACE is instead based on the unconditional simulation algorithm described in section 3.2, and kriging.

Consider a stationary random field  $Z(\mathbf{x})$ , and observations  $Z_0(\mathbf{x})$  at  $m$  locations  $\mathbf{x}_1, \dots, \mathbf{x}_m$ :  $\mathbf{Z}_0 = (Z(\mathbf{x}_1), \dots, Z(\mathbf{x}_m))'$ . Let  $\hat{Z}(\mathbf{x})$  be the predicted

## Gaussian type covariance function



## Modified Bessel covariance function

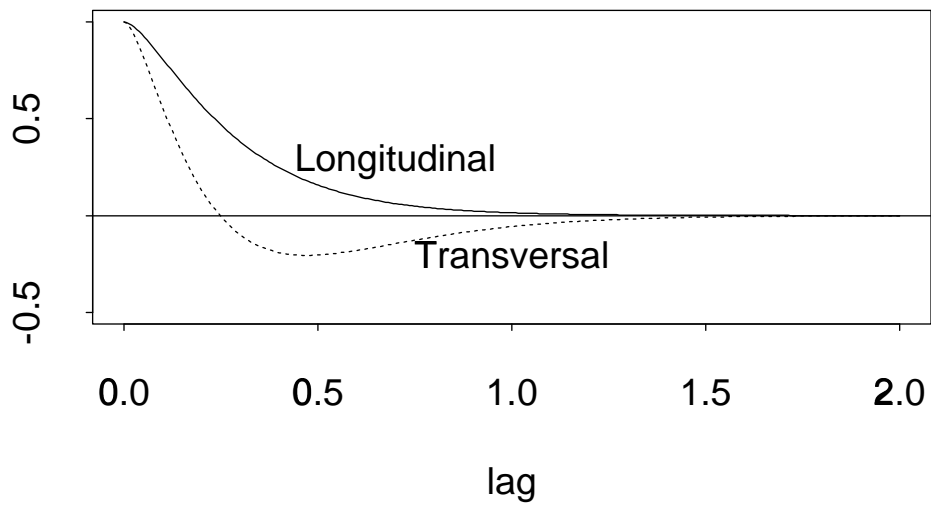


Figure 1: Transversal and longitudinal components of the “gaussian” type and modified Bessel function covariance models, with unit range.

value at  $\mathbf{x}$  based on the data  $\mathbf{Z}_0$ . We have

$$(11) \quad Z(\mathbf{x}) = \hat{Z}(\mathbf{x}) + (Z(\mathbf{x}) - \hat{Z}(\mathbf{x})).$$

Let  $Z_S(\mathbf{x})$  be an unconditional simulation of the field, and let  $\hat{Z}_S(\mathbf{x})$  be the predicted field based on the values of  $Z_S$  at locations  $\mathbf{x}_1, \dots, \mathbf{x}_m$ . We replace the error  $(Z(\mathbf{x}) - \hat{Z}(\mathbf{x}))$  in (11) by  $(Z_S(\mathbf{x}) - \hat{Z}_S(\mathbf{x}))$ . Now, the resulting random field

$$(12) \quad Z_{CS}(\mathbf{x}) = \hat{Z}(\mathbf{x}) + (Z_S(\mathbf{x}) - \hat{Z}_S(\mathbf{x}))$$

will have the same first and second order properties as the original field  $Z(\mathbf{x})$  (Ripley, 1981, pp.64-72). Also,  $Z_{CS}(\mathbf{x}_i) = Z(\mathbf{x}_i) = \mathbf{Z}_{0i}$ ;  $i = 1, \dots, m$ , so the observations are reproduced at the data locations.

Rewriting equation (12) gives

$$(13) \quad \begin{aligned} Z_{CS}(\mathbf{x}) &= Z_S(\mathbf{x}) + (\hat{Z}(\mathbf{x}) - \hat{Z}_S(\mathbf{x})) \\ &= Z_S(\mathbf{x}) + \mathbf{k}^T(\mathbf{x})\Sigma^{-1}(\mathbf{Z}_0 - \mathbf{Z}_{0S}), \end{aligned}$$

where  $\Sigma$  is the  $m$  times  $m$  covariance matrix, and  $\mathbf{k}(\mathbf{x})$  is a length  $m$  vector with elements  $C(\|\mathbf{x} - \mathbf{x}_i\|)$ ;  $i = 1, \dots, m$ .  $\mathbf{Z}_{0S}$  is the vector of unconditionally simulated values in the  $m$  locations.

Using equation (13), the conditional simulation of the field  $Z(\mathbf{x})$  is carried out by

1. unconditional simulation in the simulation domain and at the data locations, and
2. kriging prediction of the residuals  $(Z_0(\mathbf{x}_i) - Z_{0S}(\mathbf{x}_i))$ ;  $i = 1, \dots, m$ .

A *vector field* can be simulated by a direct generalization of the above method for scalar fields. Let

$$(14) \quad \mathbf{Y}(\mathbf{x}) = \begin{pmatrix} U(\mathbf{x}) \\ V(\mathbf{x}) \end{pmatrix}$$

be the vector valued random field. The components of the conditionally simulated vector field,  $U(\mathbf{x})$  and  $V(\mathbf{x})$ , can, in analogy to equation (13), be computed by

$$(15) \quad U_{CS}(\mathbf{x}) = U_S(\mathbf{x}) + \mathbf{k}_U^T(\mathbf{x})\Sigma_Y^{-1}(\mathbf{Y}_0 - \mathbf{Y}_{0S})$$

and

$$(16) \quad V_{CS}(\mathbf{x}) = V_S(\mathbf{x}) + \mathbf{k}_V^T(\mathbf{x})\Sigma_Y^{-1}(\mathbf{Y}_0 - \mathbf{Y}_{0S}),$$

where

$$(17) \quad \mathbf{k}_U(\mathbf{x}) = \begin{pmatrix} \mathbf{k}_{UU}(\mathbf{x}) \\ \mathbf{k}_{UV}(\mathbf{x}) \end{pmatrix} = \begin{pmatrix} \text{cov}(U(\mathbf{x}), U(\mathbf{x}_i))_{i=1, \dots, N(U)} \\ \text{cov}(U(\mathbf{x}), V(\mathbf{x}_j))_{j=1, \dots, N(V)} \end{pmatrix}$$

and

$$(18) \quad \mathbf{k}_V(\mathbf{x}) = \begin{pmatrix} \mathbf{k}_{VU}(\mathbf{x}) \\ \mathbf{k}_{VV}(\mathbf{x}) \end{pmatrix} = \begin{pmatrix} \text{cov}(V(\mathbf{x}), U(\mathbf{x}_i))_{i=1, \dots, N(U)} \\ \text{cov}(V(\mathbf{x}), V(\mathbf{x}_j))_{j=1, \dots, N(V)} \end{pmatrix}.$$

The numbers  $N(U)$  and  $N(V)$  are the number of conditions on the  $U$ - and  $V$ -components, respectively. The data covariance matrix  $\Sigma_Y$  is of dimension  $(N(U) + N(V), N(U) + N(V))$ , and is partitioned

$$(19) \quad \Sigma_Y = \begin{pmatrix} \Sigma_{UU} & \Sigma_{UV} \\ \Sigma_{VU} & \Sigma_{VV} \end{pmatrix}.$$

The numerical problems arising from using the Cholesky decomposition method, might cause conditionally simulated values not interpolating the data locations. The problem increases with an increasing number of points within the simulation domain, or by increasing the range of the covariance.

## 5 Examples

### 5.1 Unconditional simulation

We have simulated several realisations of non-divergent vector fields by the two methods described in section 3. The simulation domain is an equally spaced  $20 \times 20$  grid lattice on  $[0,1] \times [0,1]$ .

For the method computing the vector field by differentiation of a simulated scalar field  $\Psi$  (referred to as method 1), the scalar field is simulated from a model with covariance function

$$(20) \quad C(r) = \sigma^2 \frac{1}{2} \left( \frac{rS}{R} \right)^2 K_2 \left( \frac{rS}{R} \right)$$

where  $K_2$  is the modified Bessel function of order 2, and the parameters  $R$  and  $S$  are the range and a scaling parameter (See Abrahamsen, p.44, for a



description of the properties of covariance functions based on modified Bessel functions of general order).

One realisation of a resulting vector field is shown in figure 2.

For the direct simulation of the non-divergent vector field (method 2), we need an expression for the covariance- and cross-covariance-functions for the components of the field. Using (3), these are

$$\begin{aligned}
 F_{UU} &= \frac{1}{2}\sigma^2 \left(\frac{S}{R}\right)^3 \left(rK_1\left(\frac{rS}{R}\right) - \left(\frac{S}{R}\right)K_0\left(\frac{rS}{R}\right)r_y^2\right) \\
 (21) \quad F_{VV} &= \frac{1}{2}\sigma^2 \left(\frac{S}{R}\right)^3 \left(rK_1\left(\frac{rS}{R}\right) - \left(\frac{S}{R}\right)K_0\left(\frac{rS}{R}\right)r_x^2\right) \\
 F_{UV} &= \frac{1}{2}\sigma^2 \left(\frac{S}{R}\right)^4 K_0\left(\frac{rS}{R}\right)r_x r_y
 \end{aligned}$$

where  $r_x$  and  $r_y$  are the components of the separating vector along the two coordinate directions.

One realisation of a vector field simulated from this covariance model, and with  $\boldsymbol{\mu} = (0,0)^T$ , is shown in figure 3.

For comparison, a realisation of a non-divergent vector field, simulated by method 2 and using covariance functions derived from the covariance model defined in (10), is plotted in figure 4. If we compare this field to the one plotted in figure 3, we see that the modified Bessel function model gives a less smooth realisation.

To check that the simulated fields have the expected covariance structure, some longitudinal and transversal nonparametric semivariograms, averaged over 200 realisations, are computed. These are compared to the theoretical models. From (21) it is seen that for longitudinal ( $r_y = 0$ ) and transversal ( $r_x = 0$ ) components of the covariance, the covariance functions are independent of the direction of the separating vector  $\boldsymbol{r}$ , and the cross-covariance is zero. The semivariograms computed along these directions are therefore easy to visualize.

The nonparametric semivariograms,  $\bar{\gamma}(h)$ , where  $h$  is the lag, are computed by (Cressie, p.75)

$$(22) \quad \bar{\gamma}(h_k) = \left\{ \frac{1}{N(h_k)} \sum_{N(h_k)} |Z(\boldsymbol{x}_i) - Z(\boldsymbol{x}_j)|^{(1/2)} \right\}^4 / (0.457 + 0.494/N(h_k));$$

for  $k = 1, \dots, nl$ .  $N(h_k)$  is the number of pairs of simulated values  $Z(\boldsymbol{x})$  in lag interval number  $k$ ,  $nl$  is the number of lags, and the sum is over all pairs of simulated values with intermediate distance in lag interval  $k$ .

Plots of longitudinal and transversal average semivariograms along four horizontal directions are shown in figures 5 and 6 for method 1, and figures 7 and 8 for method 2.

The estimated semivariograms for method 1, seem to have a somewhat longer range than what is defined in the specification of the model. This can be related to the numerical differentiation (4) of the simulated scalar field. The derivation algorithm has an effect similar to that of a filter, and a smoothing of the field is introduced. We suppose that this effect will be reduced by using a more dense grid lattice.

## 5.2 Conditional simulation

As suggested in section 2, the nondivergent vector field can be thought of as a fluid velocity field. As an example, consider a velocity field that is to be simulated on an equally spaced 20 x 20 grid on  $[0,1] \times [0,1]$ , under the condition of zero perpendicular velocity at the upper and lower boundaries, say  $V(\mathbf{x}, 0) = 0$  and  $V(\mathbf{x}, 1) = 0$ .

We have simulated 200 realisations of such a field, using the same model as for the unconditional simulation presented in the previous section.

A realisation is shown in figure 9. As for the unconditional simulations, we have computed longitudinal and transversal semivariograms, to check the correspondence to the theoretical model. These semivariograms are plotted in figures 10 and 11.

The variance for the transversal component tends to zero when approaching the lines  $y = 0$  and  $y = 1$  because  $V(x, 0) = 0$  and  $V(x, 1) = 0$ . The variance of the  $U$ -component of the vector field seems unaffected by the conditions on the  $V$ -component. This is because the transversal and longitudinal velocity components are uncorrelated for a non-divergent field.

## Differentiation of scalar field, modified Bessel covariance

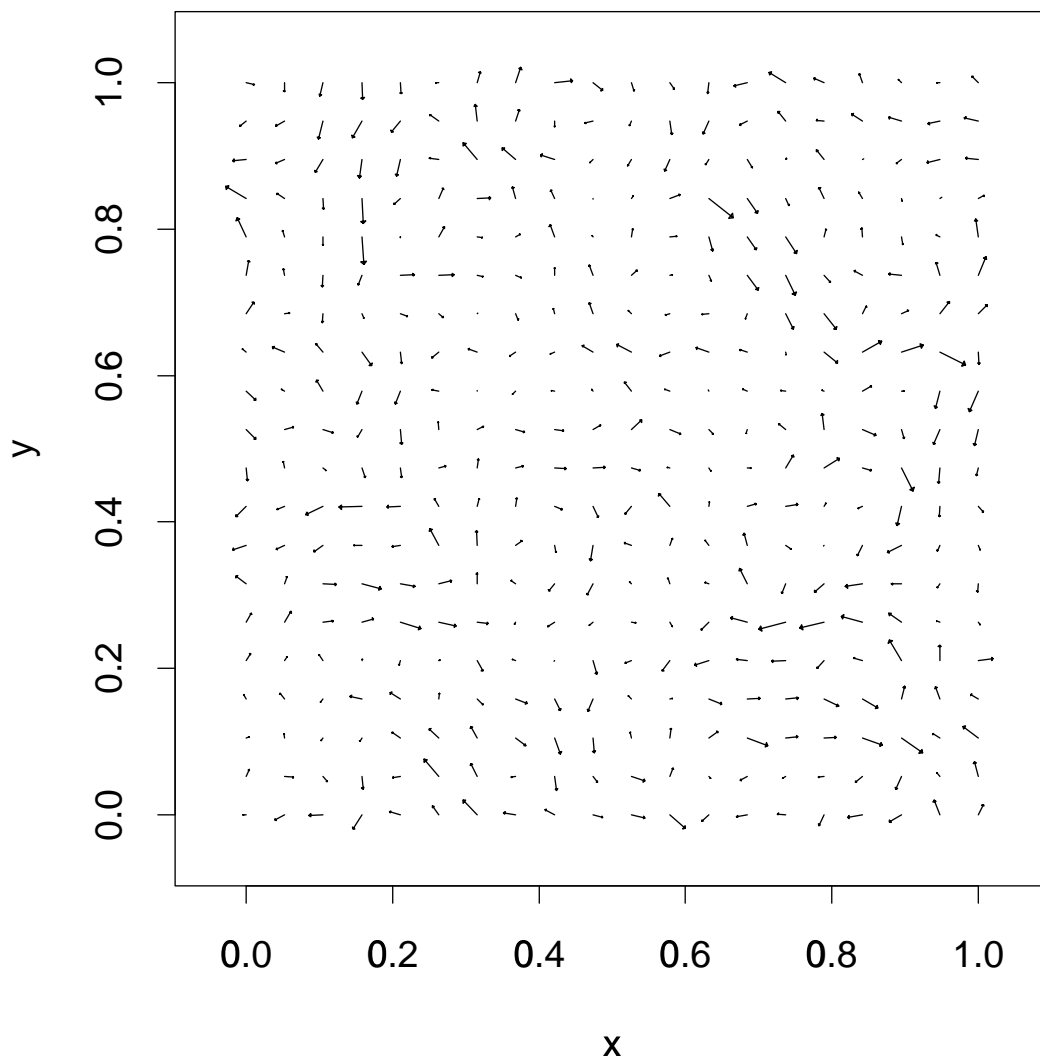


Figure 2: A realisation of a vector field, computed by differentiation of a simulated scalar field. The scalar field is simulated using the modified Bessel function covariance model (20) with range  $R = 0.33$  and unit variance.

## Direct simulation, modified Bessel covariance

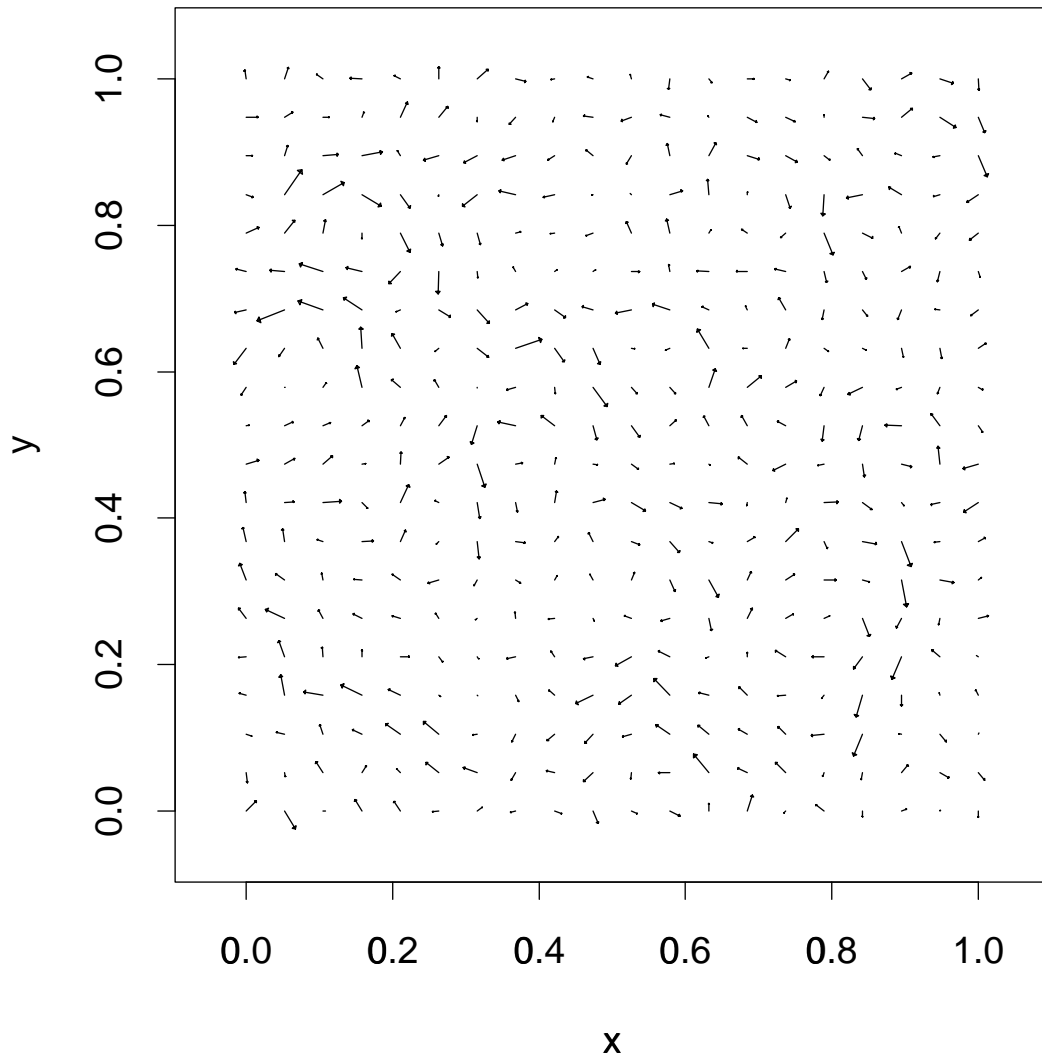


Figure 3: A realisation of a vector field, computed by direct simulation using the modified Bessel function covariance model (21) with range  $R = 0.33$  and unit variance.

## Direct simulation, gaussian type covariance

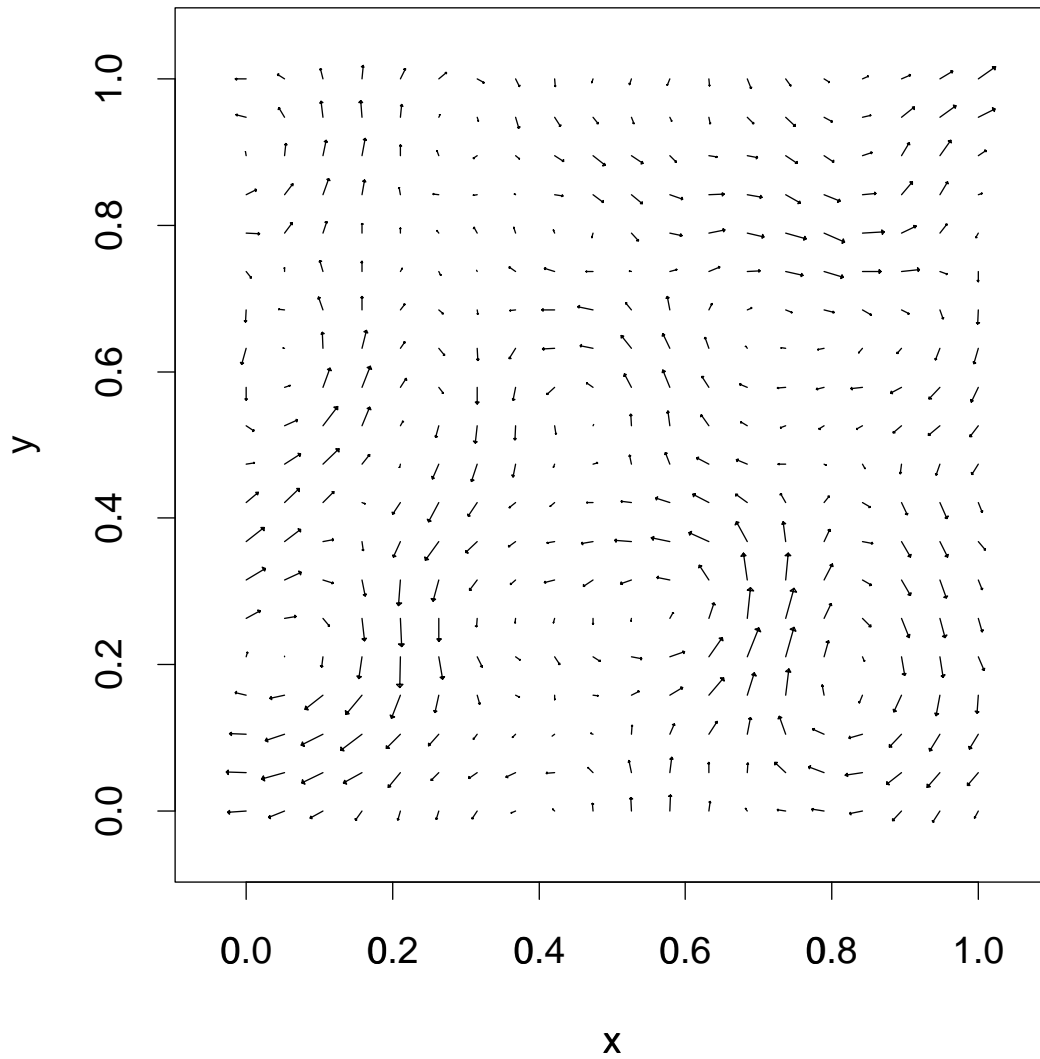


Figure 4: A realisation of a vector field, computed by direct simulation using the “gaussian” type covariance model (10) with range  $R = 0.33$  and unit variance.

# Longitudinal semivariograms, diff. of scalar field

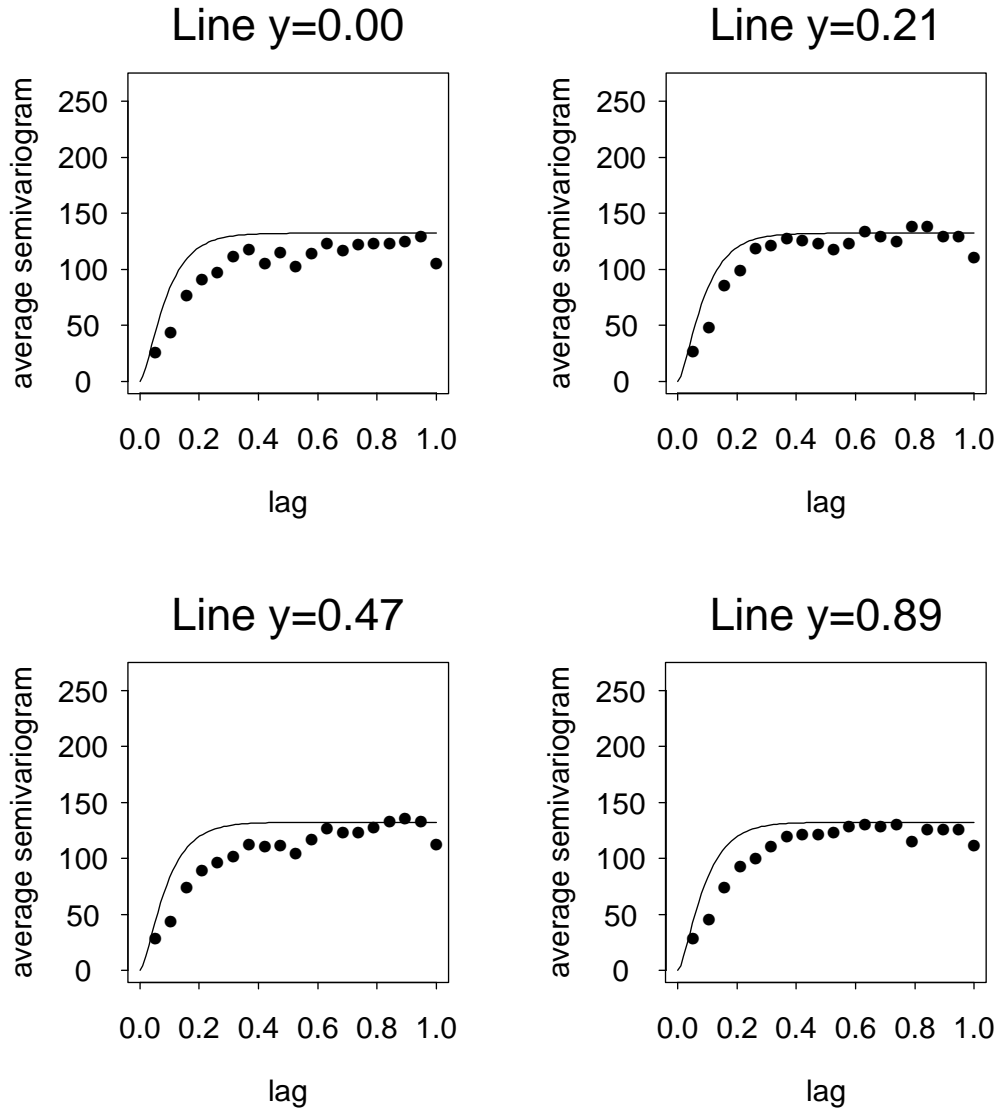


Figure 5: Longitudinal semivariograms for grid points at lines  $y=0.0$ ,  $y=0.21$ ,  $y=0.47$  and  $y=0.89$ , for the field simulated by method 1. The semivariograms are averaged over 200 simulations. The solid lines are the theoretical model, using the modified Bessel function covariance model, with range  $R = 0.33$  and unit variance.

# Transversal semivariograms, diff. of scalar field

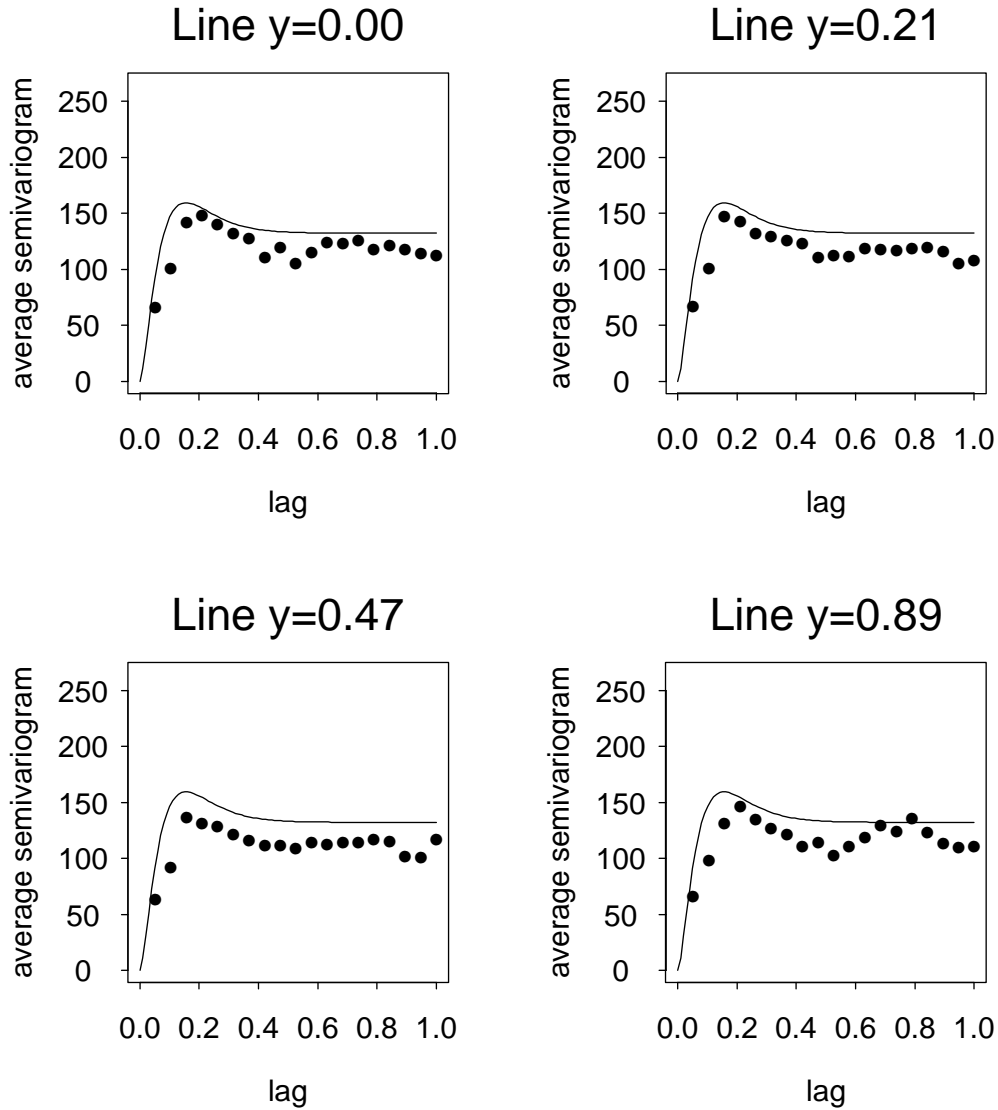


Figure 6: Transversal semivariograms for grid points at lines  $y=0.0$ ,  $y=0.21$ ,  $y=0.47$  and  $y=0.89$ , for the field simulated by method 1. The semivariograms are averaged over 200 simulations. The solid lines are the theoretical model, using the modified Bessel function covariance model, with range  $R = 0.33$  and unit variance.

# Longitudinal semivariograms, direct simulation

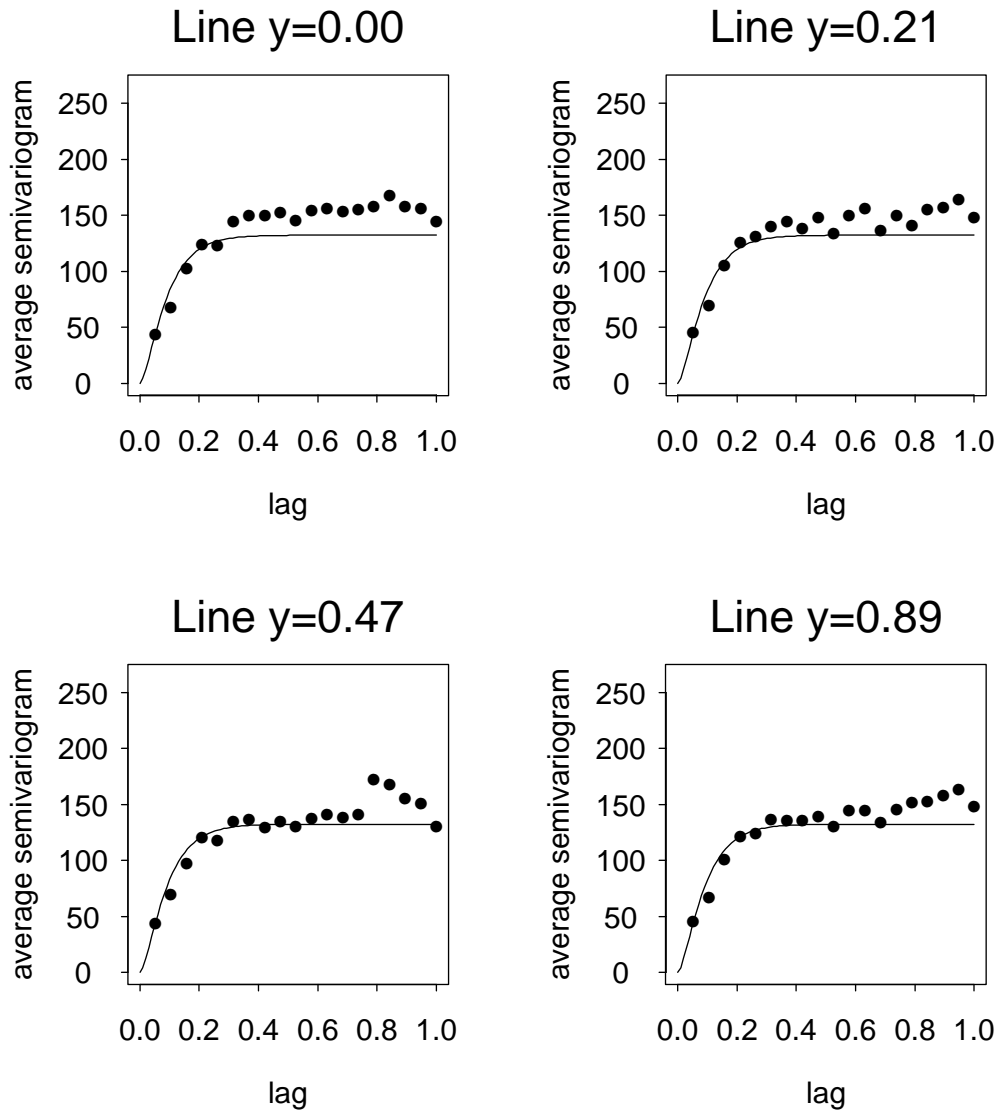


Figure 7: Longitudinal semivariograms for grid points at lines  $y=0.0$ ,  $y=0.21$ ,  $y=0.47$  and  $y=0.89$ , for the field simulated by method 2. The semivariograms are averaged over 200 simulations. The solid lines are the theoretical model, using the modified Bessel function covariance model, with range  $R = 0.33$  and unit variance.



# Transversal semivariograms, direct simulation

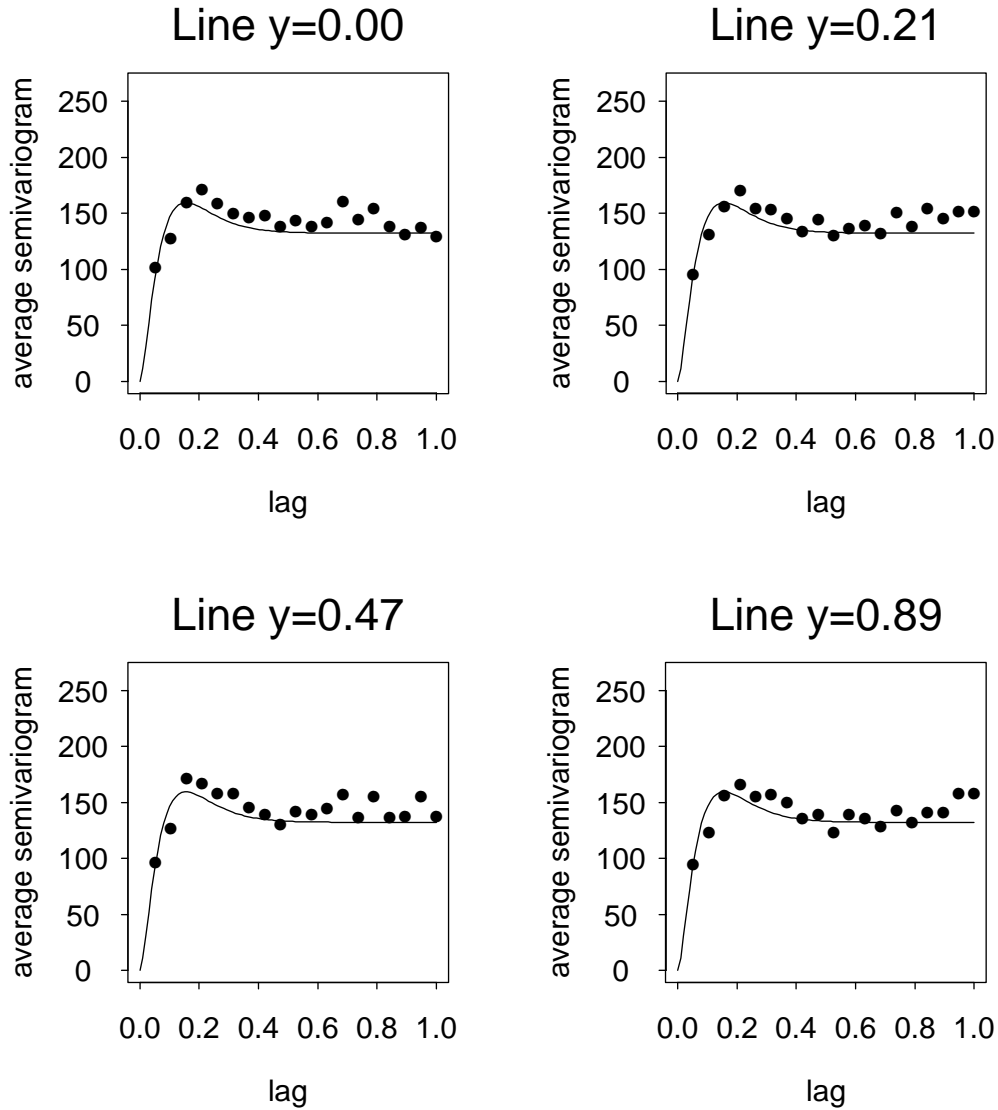


Figure 8: Transversal semivariograms for grid points at lines  $y=0.0$ ,  $y=0.21$ ,  $y=0.47$  and  $y=0.89$ , for the field simulated by method 2. The semivariograms are averaged over 200 simulations. The solid lines are the theoretical model, using the modified Bessel function covariance model, with range  $R = 0.33$  and unit variance.

## Conditional simulation, modified Bessel covariance

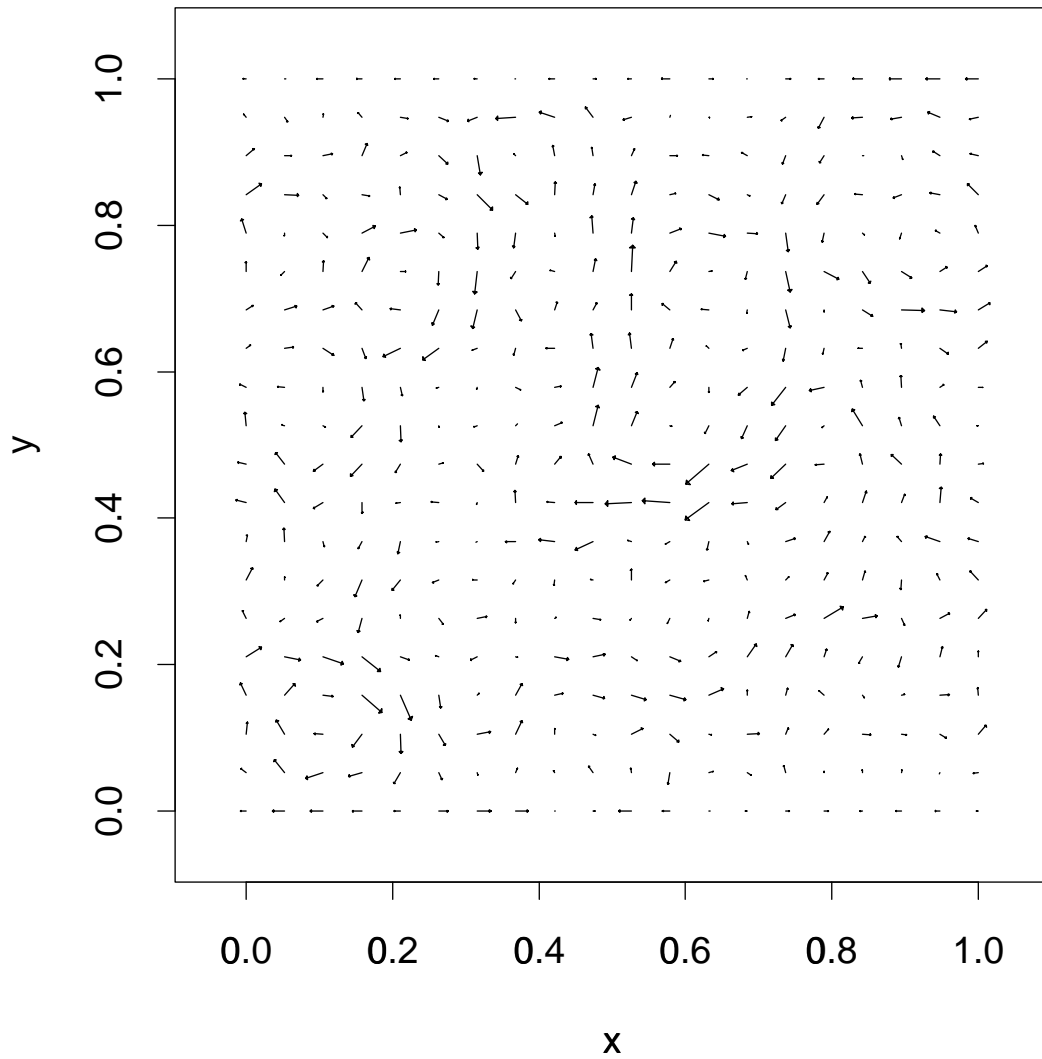


Figure 9: A realisation of a vector field, computed by conditional simulation using the modified Bessel function covariance model (21) with range  $R = 0.33$  and unit variance.

# Longitudinal semivariograms conditional simulation

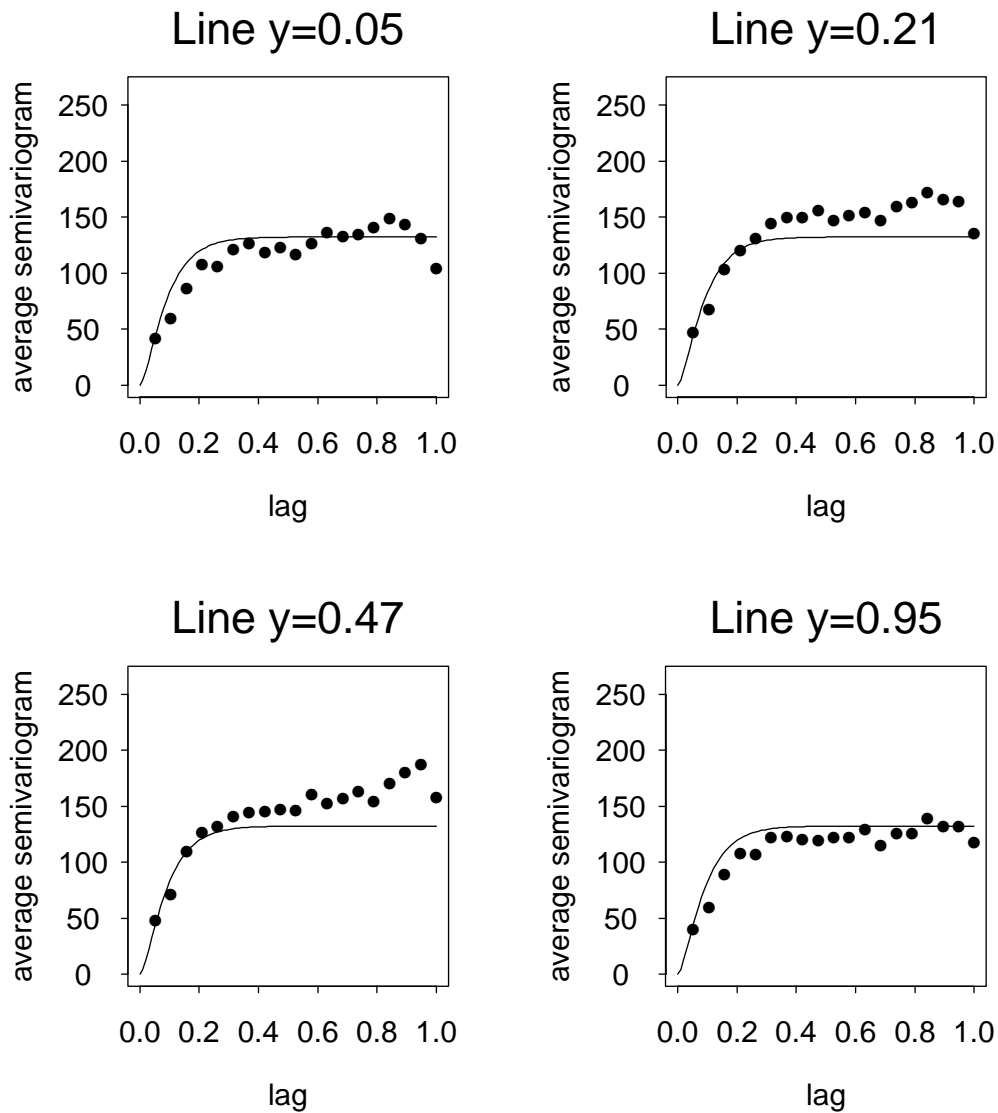


Figure 10: Longitudinal semivariograms for grid points at lines  $y=0.05$ ,  $y=0.21$ ,  $y=0.47$  and  $y=0.95$ , for the field computed by conditional simulation. The semivariograms are averaged over 200 simulations. The solid lines are the theoretical model, using the modified Bessel function covariance model, with range  $R = 0.33$  and unit variance.

# Transversal semivariograms conditional simulation

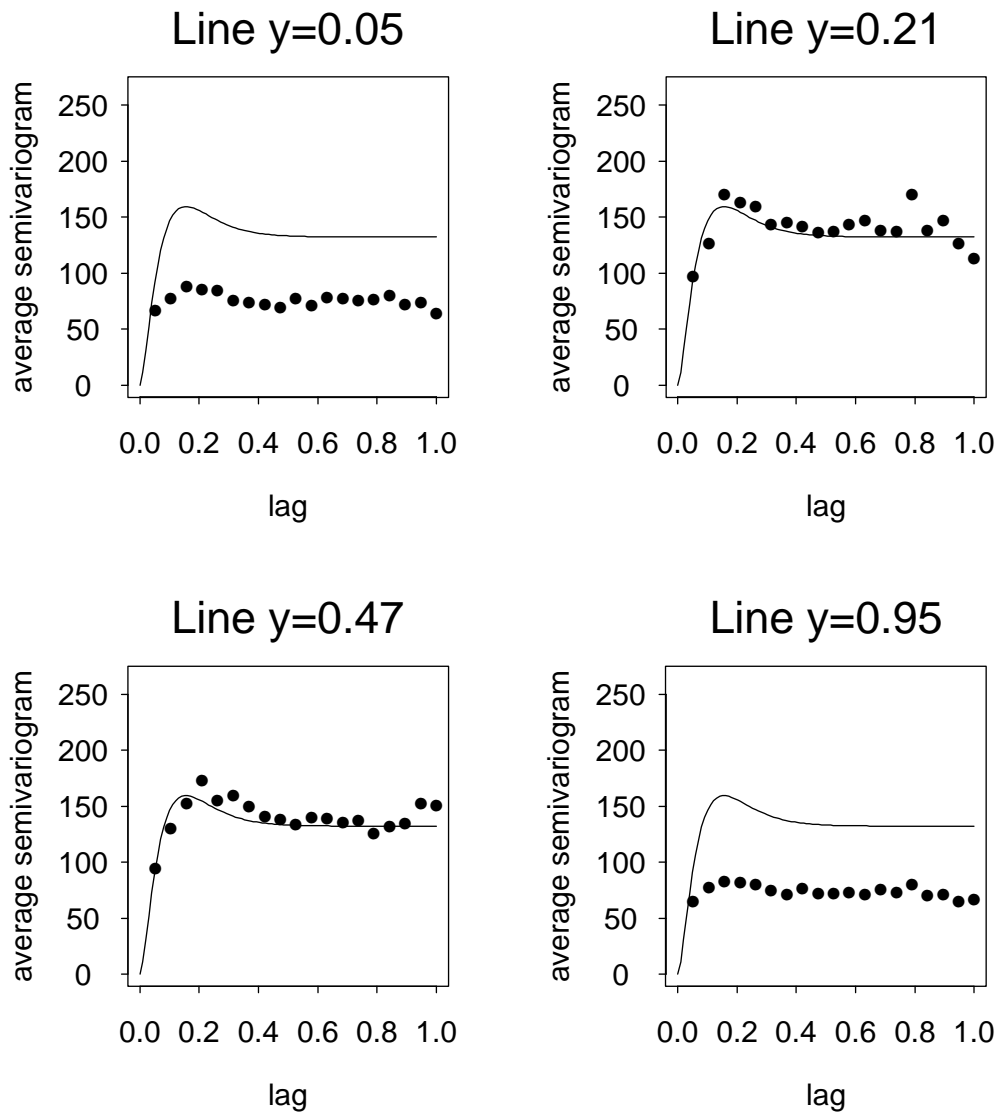


Figure 11: Transversal semivariograms for grid points at lines  $y=0.05$ ,  $y=0.21$ ,  $y=0.47$  and  $y=0.95$ , for the field computed by conditional simulation. The semivariograms are averaged over 200 simulations. The solid lines are the theoretical model, using the modified Bessel function covariance model, with range  $R = 0.33$  and unit variance.

## 6 Verification of the program by simulation

The aim of this section is to check that a realisation of a stochastic vector field, simulated conditionally by the method implemented in NSPACE, has the correct covariance structure.

Consider the example described in section 5.2. In this section, we will use the same model, but the simulation domain,  $D$ , will be reduced to an equally spaced  $5 \times 5$  grid on  $[0, 1] \times [0, 1]$ , instead of the  $20 \times 20$  grid of section 5.2. The parameters of the covariance function (20) are set to  $R = 1$  and  $\sigma^2 = 1$ .

We consider the non-divergent random vector field

$$\{U(\mathbf{x}, \mathbf{y}), V(\mathbf{x}, \mathbf{y}); (\mathbf{x}, \mathbf{y}) \in D\},$$

simulated conditionally on  $V(\mathbf{x}, 0) = V(\mathbf{x}, 1) = 0$ . Arrange the components of  $U$  and  $V$  into a vector

$$Z = \{U(0, 0), U(0.25, 0), \dots, U(1, 1), V(0, 0), V(0.25, 0), \dots, V(1, 1)\}.$$

Partition  $Z$  into  $(Z_1, Z_2)$ , where

$$Z_1 = \{V(0, 0), V(0.25, 0), \dots, V(1, 0), V(0, 1), V(0.25, 1), \dots, V(1, 1)\}$$

and

$$(23) \quad \begin{aligned} Z_2 = & \{U(0, 0), U(0.25, 0), \dots, U(1, 1), \\ & V(0, 0.25), V(0.25, 0.25), \dots, V(1, 0.75)\}. \end{aligned}$$

Now,  $Z_1$  consists of the 10 components of  $Z$  with conditions, and  $Z_2$  consists of the remaining 40 components of  $Z$ . The covariance matrix of  $Z_2$  given  $Z_1$  is

$$(24) \quad \Sigma_{Z_2|Z_1} = \Sigma_{Z_2} - \Sigma_{Z_2, Z_1} \Sigma_{Z_1, Z_1}^{-1} \Sigma_{Z_1, Z_2}.$$

To check that a realisation of the conditionally simulated stochastic field has the correct covariance structure, 1000 realisations of  $Z_2$  given  $Z_1$  are simulated. Then, the sample covariance matrix of  $Z_2$  given  $Z_1$  is compared to the theoretical covariance matrix.

The covariance matrix of  $\mathcal{W} = \Sigma_{Z_2|Z_1}^{-1/2} Z_2$  is the identity matrix. Denote the sample covariance matrix of  $\mathcal{W}$  by  $\hat{\Sigma}_{\mathcal{W}}$ , and consider

$$(25) \quad M = \sqrt{1000}(\hat{\Sigma}_{\mathcal{W}} - I),$$

where  $I$  is the identity matrix. Now, each element of  $M$  has expectation zero. Also, the diagonal elements of  $M$  have variance 2 and the non-diagonal

elements have variance 1. This can be exploited to assess the deviation of  $\hat{\Sigma}_{\mathcal{W}}$  from  $I$ .

The sample mean and variance of the diagonal elements of  $M$  are 0.266 and 1.270, and the corresponding values for the off-diagonal elements are  $-0.0279$  and 1.017.

The matrix  $M' = \frac{1000}{\sqrt{999}}(\hat{\Sigma}_{\mathcal{W}} - I) \approx M$  will be Wishart distributed,

$$M' \sim W_{40}(I, 999).$$

For the diagonal elements of  $M$  we have

$$\sqrt{1000} * \text{diag}(M)_i \sim 1.0 * \chi_{999}^2.$$

Figure 12 shows a Q-Qplot of the elements of  $\text{diag}(M)$  vs. quantiles of the  $1/\sqrt{999} * \chi_{999}^2$ -distribution.

Histograms of the off-diagonal elements,  $M_{ij}$ ;  $i \neq j$ , and the diagonal elements of  $M$  are shown in figure 13.

The sample variance of the diagonal elements is quite small, compared to the expected value, which is 2. Also, the Q-Qplot seems to deviate from the line  $y = x$ . To get an indication of the magnitude of the simulation variance, 1000 realisations of a multionormal model, with covariance matrix (24), are simulated 4 times. The sample mean and variance of  $\text{diag}(M)$  are computed for each run, and some results are listed in table 1.

Run	Sample mean	Sample variance
1	-0.0137	2.201
2	-0.236	2.667
3	-0.0636	1.843
4	-0.0029	1.573

Table 1: Sample mean and variance for the diagonal of  $M$  in (25), for 4 realisations of a series of 1000 simulations from a conditional multinormal distribution.

On the basis of these investigations, the conditional simulation module of NSPACE seems correct.

## Q-Q plot for diagonal of sample covariance matrix

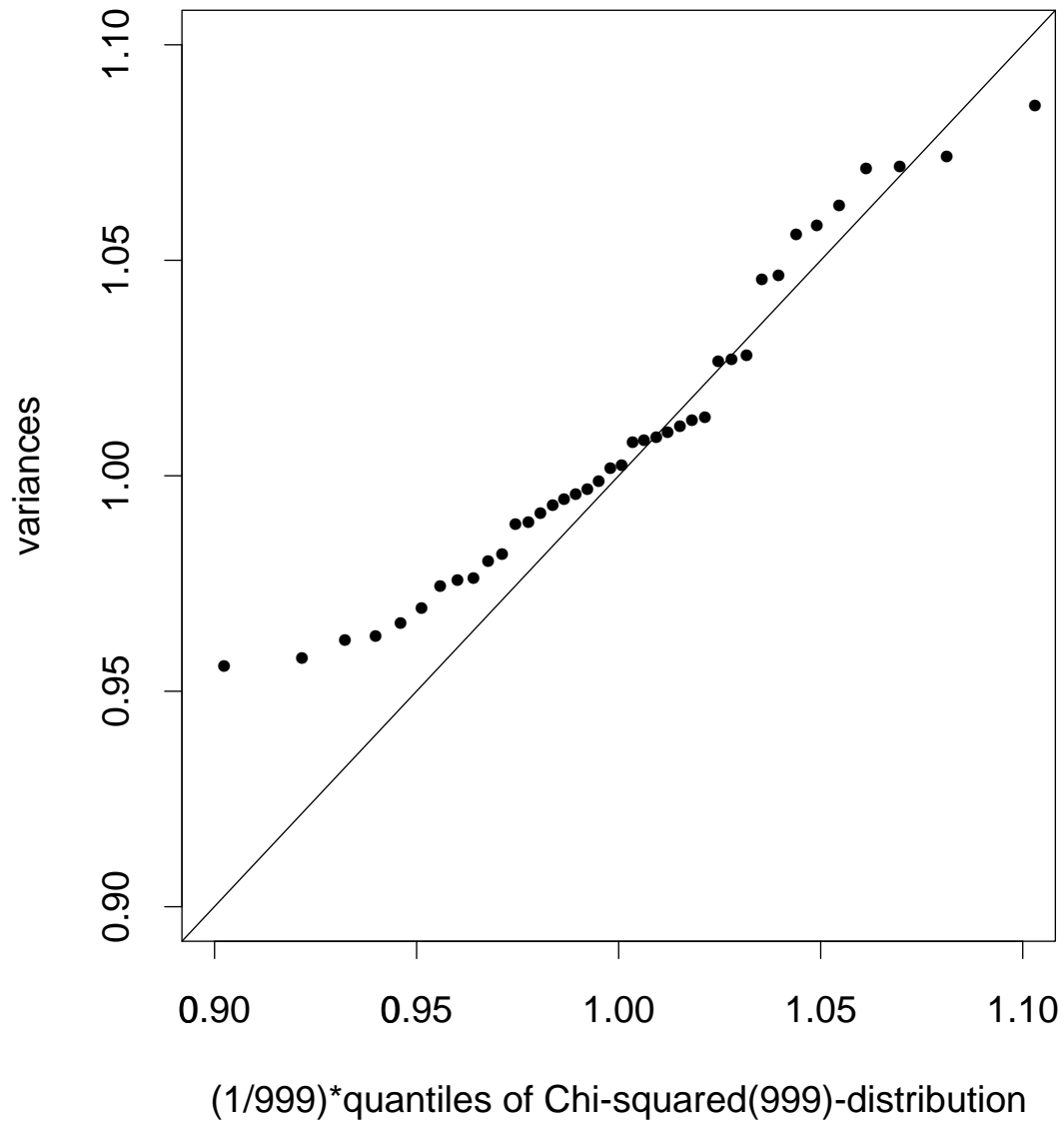


Figure 12: Q-Qplot for diagonal elements of the standardized sample covariance matrix,  $M$ , vs. quantiles of the  $1/\sqrt{999} * \chi_{999}^2$ -distribution. The solid line is the line  $y = x$ . A line fitted by least squares to the Q-Qplot, has slope 0.78 and intercept 0.23.

## Elements of sample covariance matrix

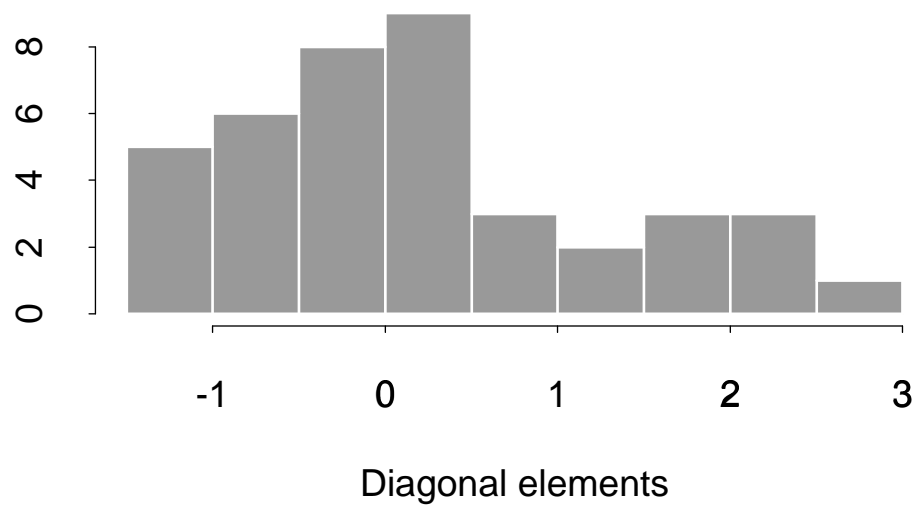
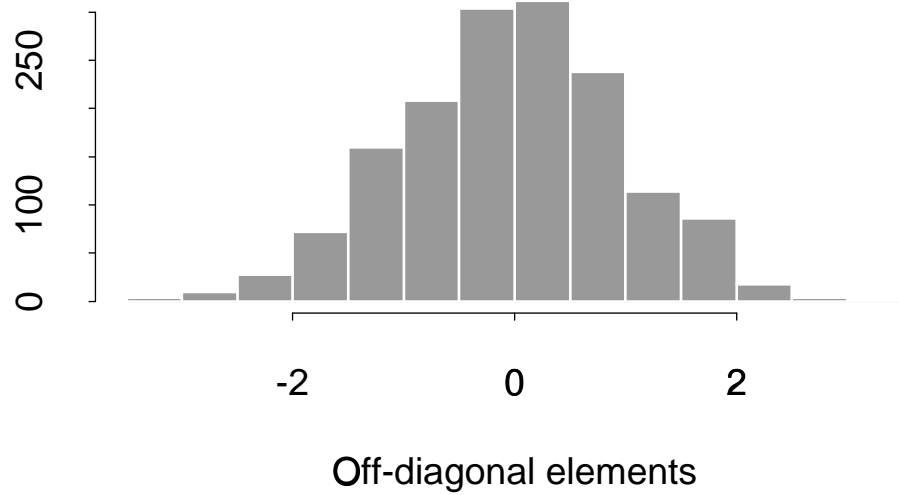


Figure 13: Histograms of the off-diagonal and diagonal elements of the standardized sample covariance matrix  $M$ .



## 7 Conclusions

We have described the methods for unconditional and conditional simulation of non-divergent vector fields in NSPACE. The methods are based on Cholesky decomposition of a covariance matrix. Since this decomposition is computationally expensive, these methods are suitable only for relatively small problems. Methods based on the Fourier transform or the turning bands method are probably more suitable for large problems. The Cholesky decomposition method is also sensitive to the smoothness of the field to be simulated. This problem can be resolved by choosing carefully among valid covariance models. A covariance model based on modified Bessel functions has been shown to have desirable properties in that respect.

## 8 References

Abrahamsen, P.: “A Review of Gaussian Random Fields and Correlation Functions”, NR-report no.878, 1994.

Høst, G.: “A Note on Two-Dimensional Non-Divergent Gaussian Random Vector Fields.”, NR-note STAT/05/1994.

Ripley, B.D.: “Spatial Statistics”, Wiley, 1981.